

1 Track reconstruction at the LUXE experiment using quantum algorithms

2 ARIANNA CRIPPA<sup>1,2</sup>, LENA FUNCKE<sup>3</sup>, TOBIAS HARTUNG<sup>4,5</sup>, BEATE HEINEMANN<sup>6,7</sup>,  
3 KARL JANSEN<sup>1</sup>, ANNABEL KROPF<sup>6,7</sup>, STEFAN KÜHN<sup>4</sup>, FEDERICO MELONI<sup>6</sup>, DAVID  
4 SPATARO<sup>6,7</sup>, CENK TÜYSÜZ<sup>1,2</sup> AND YEE CHINN YAP<sup>6</sup>

5 <sup>1</sup> *Deutsches Elektronen-Synchrotron DESY, Platanenallee 6, 15738 Zeuthen, Germany*

6 <sup>2</sup> *Institut für Physik, Humboldt-Universität zu Berlin, Newtonstr. 15, 12489 Berlin,*  
7 *Germany*

8 <sup>3</sup> *Center for Theoretical Physics, Co-Design Center for Quantum Advantage, and NSF AI*  
9 *Institute for Artificial Intelligence and Fundamental Interactions, Massachusetts Institute*  
10 *of Technology, 77 Massachusetts Avenue, Cambridge, MA 02139, USA*

11 <sup>4</sup> *Computation-Based Science and Technology Research Center, The Cyprus Institute, 20*  
12 *Kavafi Street, 2121 Nicosia, Cyprus*

13 <sup>5</sup> *University of Bath, Claverton Down, Bath BA2 7AY, UK*

14 <sup>6</sup> *Deutsches Elektronen-Synchrotron DESY, Notkestr. 85, 22607 Hamburg, Germany*

15 <sup>7</sup> *Physikalisches Institut, Albert-Ludwigs-Universität Freiburg, Hermann-Herder-Str. 3a,*  
16 *79104 Freiburg, Germany*

17 ABSTRACT

18 LUXE (Laser Und XFEL Experiment) is a proposed experiment at DESY which  
19 will study Quantum Electrodynamics (QED) in the strong-field regime, where  
20 QED becomes non-perturbative. The measurement of the rate of  
21 electron-positron pair creation, an essential ingredient to study this regime, is  
22 enabled by the use of a silicon tracking detector. Precision tracking of positrons  
23 traversing the four layers of the tracking detector becomes very challenging at  
24 high laser intensities due to the high rates, which can be computationally  
25 expensive for classical computers. In this paper, a preliminary study of the  
26 potential of quantum computers to reconstruct positron tracks is presented. The  
27 reconstruction problem is formulated in terms of a Quadratic Unconstrained  
28 Binary Optimisation (QUBO), and solved using simulated quantum computers  
29 and hybrid quantum-classical algorithms such as Variational Quantum  
30 Eigensolver (VQE). Different ansatz circuits and optimisers are studied. The  
31 results are discussed and compared with classical track reconstruction algorithms  
32 using Graph Neural Network and Combinatorial Kalman Filter.

33 PRESENTED AT

34 Connecting the Dots Workshop (CTD 2022)  
35 May 31 - June 2, 2022

## 1 Introduction

LUXE [1] is a planned experiment at DESY in Hamburg to study the transition far into the strong-field regime of QED, where QED becomes non-perturbative. In this experiment, the high-energy electron beam from the European XFEL is used together with a high-power laser. Both the interaction of the laser beam with the electron beam as well as with a beam of bremsstrahlung photons are studied. Processes of interest are Compton scattering and Breit-Wheeler pair creation. In the Compton process in a plane wave background of a laser field,

$$e^- + n\gamma_L \rightarrow e^- + \gamma, \quad (1)$$

an electron emits a high-energy photon, where  $n$  is the number of laser photons  $\gamma_L$  participating in the process. Breit-Wheeler pair creation,

$$\gamma + n\gamma_L \rightarrow e^+ + e^-, \quad (2)$$

in the presence of a strong electromagnetic field is the decay of a high energy photon into electron-positron pairs. The classical non-linearity parameter,

$$\xi = \frac{m_e \mathcal{E}_L}{\omega_L \mathcal{E}_{cr}}, \quad (3)$$

with  $m_e$  as the electron mass,  $\omega_L$  as the laser frequency,  $\mathcal{E}_L$  as the instantaneous laser field strength and  $\mathcal{E}_{cr} = m_e^2 c^3 / e\hbar$  as the critical field strength, known as Schwinger-Limit, is used to demarcate the regime of strong-field QED in particle-laser and photon-laser interactions ( $\xi \gg 1$ ).

## 2 Experimental setup

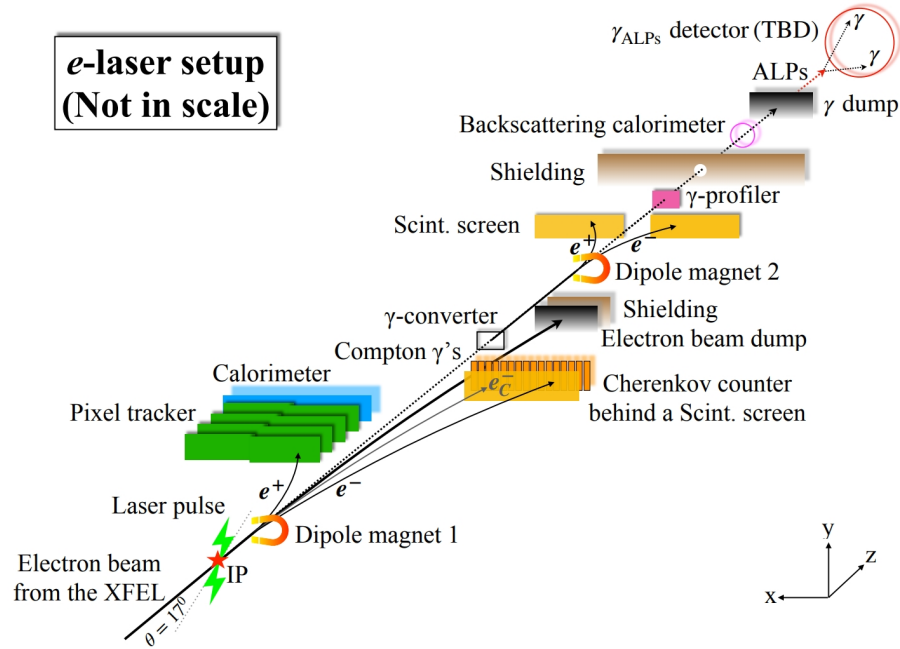


Figure 1: LUXE setup in  $e$ -laser mode. Recreated from [1].

Figure 1 shows the experimental setup of LUXE for the  $e$ -laser mode. The electron beam from the European XFEL is guided to the interaction point (IP) and crossed with the high-power laser. In the initial phase-0 of LUXE, a laser with 40 TW is used. For phase-1, an upgrade of the laser up to 350 TW is

54 planned. Utilising a dipole magnet, electrons and positrons are deflected to their respective detector systems  
 55 for energy and position measurements. The track reconstruction study which is presented in the following  
 56 focuses on positrons detected by a silicon pixel tracking detector. The tracking detector system consists of  
 57 eight staves partially overlapping and forming four layers with respect to the beam-axis. Each layer covers a  
 58 length of approximately. 50 cm in x-direction. The staves are populated by 9 sensor chips, each containing  
 59  $1024 \times 512$  pixels with a size of  $29 \times 27 \mu\text{m}^2$ .

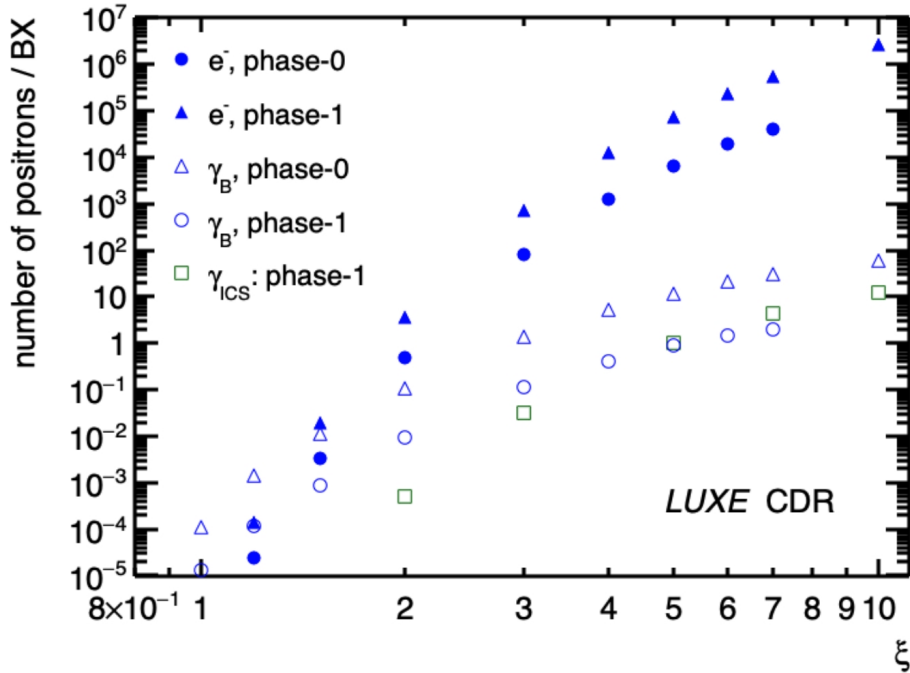


Figure 2: Number of expected positrons per interaction (BX) of the laser with both the electron beam and the Bremsstrahlung photon source as a function of the classical nonlinearity parameter  $\xi$ . Reproduced from [1].

60 To study the transition far into the non-perturbative regime of QED, a key concept is to measure the  
 61 number of positrons generated from the Breit-Wheeler process with respect to the parameter  $\xi$ . The number  
 62 of expected positrons ranges from less than  $10^{-4}$  up to  $10^6$  in the  $e$ -laser setup, displayed in Figure 2. Both  
 63 a low background rate ( $< 10^{-3}$ ) at low  $\xi$  and good linearity up to a high multiplicity are essential for track  
 64 reconstruction. For this challenging task, we explore the potential of using quantum computing algorithms  
 65 for track reconstruction. Previous results of our work can be found in Ref. [2]. An overview of possible  
 66 quantum algorithms suitable for charged particle tracking is given in Ref. [3].

### 67 3 Data sets and selection

68 In this study simulated data are used. Signal interactions at the IP are generated with PTARMIGAN [4], a  
 69 custom Monte Carlo event generator. Positrons stemming from PTARMIGAN are propagated through the  
 70 dipole magnet and the positron tracking system using a simplified simulation. In the simplified simulation,  
 71 parameters such as position and resolution of detector layers, as well as scattering processes can be tuned to  
 72 explore the impact on the tracking approach. Within the frame of this study the detector geometry of the  
 73 simplified simulation is reduced to a set of four non-overlapping layers.

74 The used simulated data predicts future measurements of phase-0 of LUXE for the  $e$ -laser setup for  $\xi \in$   
 75  $\{4, 5, 7\}$ , which corresponds to 800 to 60,000 expected positrons. Only the 500 particles per laser beam

76 interaction that are closest to the beamline are considered for the track reconstruction task in order to  
 77 equalize the size of all used data sets. Both the track density and the complexity of the track reconstruction  
 78 task increase with  $\xi$ .

79 Our starting point for track reconstruction is either doublet or triplets. Doublets are a set of two hits  
 80 from exclusively consecutive layers, while triplets are a set of two doublets with exactly one shared hit. With  
 81 respect to the beam line, an angle-based pre-selection procedure is applied to the doublets based on the  
 82 experiment geometry. Triplets are formed if the angles between two doublets with one shared hit are not  
 83 exceeding the expected maximum multiple scattering in the detector. In this procedure, the combinatorial  
 84 candidates are reduced without lowering the efficiency.

## 85 4 Methodology

### 86 4.1 Classical tracking

87 As a benchmark a classical tracking approach with a combinatorial Kalman Filter (CKF) technique is used.  
 88 For this, the A Common Tracking Software (ACTS) toolkit [5] is employed. Triplets are used as seeds to  
 89 find an initial estimate of the track parameters. Scanning for matching hit candidates, the initial estimate  
 90 is updated and the measurement search is performed at the same time. Eventually, after track finding and  
 91 fitting is completed, an ambiguity-solving step is applied to remove tracks with shared hits.

### 92 4.2 Graph neural network

93 Another method which is explored in this work is the use of a graph neural network (GNN) [6, 7]. Hits are  
 94 represented as nodes. Edges are connections between nodes, forming doublet-like structures, called segments,  
 95 and are only kept if they satisfy the pre-selection criteria. The GNN consists of alternating EdgeNetwork  
 96 and NodeNetwork and is trained to optimize the edge connections, thus learning which segments should be  
 97 chosen to be a part of track candidates. Furthermore, there is a hybrid quantum-classical version of the  
 98 GNN-based tracking [8], but this is not examined in this work.

### 99 4.3 Quantum algorithm

100 When using the quantum algorithm, the tracking task is approached by first encoding triplets as binary  
 101 variables and then deciding which triplets to keep or discard in the subsequent track reconstruction process.  
 102 An objective function is defined, called quadratic unconstrained binary optimization (QUBO), similar to  
 103 Ref. [9]. The goal is to minimise the objective

$$O = \sum_i^N \sum_{j<i} b_{ij} T_i T_j + \sum_{i=1}^N a_i T_i, \quad T_i, T_j \in \{0, 1\}, \quad (4)$$

104 with  $T_i$  and  $T_j$  representing triplets on position  $i$  and  $j$  of a possible solution vector, and  $a_i$  and  $b_{ij}$  as  
 105 coefficients.

106 The quadratic term describes the relation between triplets. This relation is quantified by the parameter  
 107  $b_{ij}$ , which has a negative value if triplets form a track candidate, a positive value if they are in conflict and  
 108 zero if they do not share a hit. The parameter  $a_i$  rates a triplet based on the angle between the two doublets  
 109 that make up the triplet. In contrast to our previous results, we are focusing entirely on the relation term  
 110 in this work, discarding the linear term completely.

111 Solving the QUBO directly on a quantum device is not possible, therefore the objective has to be mapped  
 112 to an Ising hamiltonian. Finding the ground state of the Ising hamiltonian is equivalent to minimizing the  
 113 QUBO and thus finding an optimal solution to the track reconstruction task. The Ising Hamiltonian,

$$\mathcal{H} = - \sum_{n=1}^N \sum_{m<n} \bar{b}_{nm} \sigma_n^x \sigma_m^x - \sum_{n=1}^N \bar{a}_n \sigma_n^x, \quad (5)$$

114 is solved using the Variation Quantum Eigensolver (VQE), a hybrid quantum-classical algorithm. For this  
 115 task, the Qiskit [10] toolkit is employed. As a benchmark for VQE, an analytical solution can be obtained by  
 116 using Numpy Eigensolver. In this study noise is excluded for VQE. As optimiser the Nakanishi-Fujii-Todo  
 117 (NFT) [11] algorithm is selected.

118 We have improved VQE's hyperparameters to boost performance compared to our previous results. NFT  
 119 is chosen instead of Constrained Optimization by Linear Approximation (COBYLA). The quantum circuit  
 120 following the *TwoLocal* ansatz scheme is altered to a linear entanglement from a circular entanglement  
 121 scheme. The circuit depth is increased to three (see previous results in [2]).

122 The quantum circuit is shown in Fig. 3.

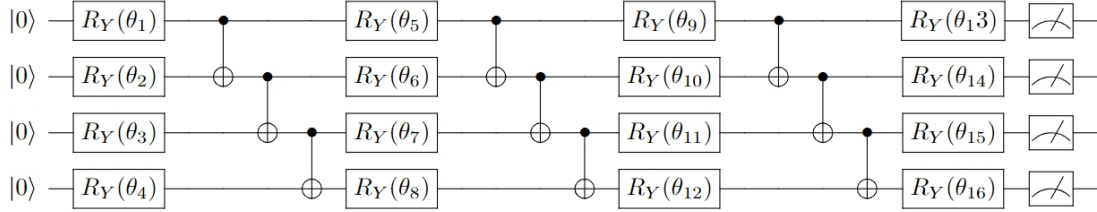


Figure 3: Variational quantum circuit layout. The *TwoLocal* ansatz is used with three repetitions of  $R_Y$  and CNOT gates for entanglement and an additional final rotation layer. For simplicity, only a four qubit system is shown.

123 To solve the QUBO an initial guess of the solution in the form of a string representation of the set  
 124 of triplets, assuming values  $\{0, 1\}$  is made. For solving the QUBO in one step, the number of available  
 125 qubits for the computation has to be the same as the number of triplets participating in the QUBO. Since  
 126 sizes of quantum devices of this magnitude are not available and simulating huge devices is computationally  
 127 infeasible, the problem has to be broken down into smaller parts, called sub-QUBOs, which are solved  
 128 sequentially in each iteration. A sub-QUBO size of 7 is chosen. The order of triplets used in the sub-QUBO  
 129 process is determined by their impact on the Hamiltonian energy if the binary representation of the triplet  
 130 in the QUBO is flipped. A sketch of the QUBO solving process with a focus on the sub-QUBO routine is  
 131 shown in Fig. 4.

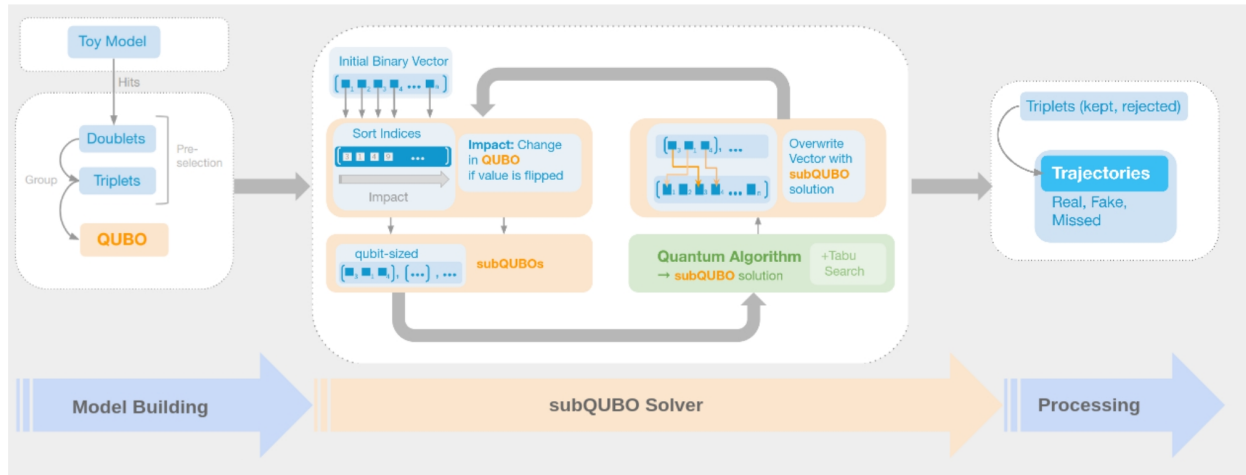


Figure 4: Sketch of the QUBO solving approach with focus on the sub-QUBO routine [2].

## 5 Results

Comparing the performance of the track reconstruction approaches is done on track level. Efficiency and fake rate are used as metrics. A track is defined as a set of four hits of consecutive layers which is either combining doublets and triplets into quadruplets or is found directly with the classical CKF-based tracking method. A matched track stems from exactly one particle.

Efficiency and fake rate are defined as

$$\text{Efficiency} = \frac{N_{\text{tracks}}^{\text{matched}}}{N_{\text{tracks}}^{\text{generated}}} \quad \text{and} \quad \text{Fake rate} = \frac{N_{\text{tracks}}^{\text{fake}}}{N_{\text{tracks}}^{\text{reconstructed}}}. \quad (6)$$

In Fig. 5 efficiency and fake rate for 500 tracks is displayed as a function of the classical non-linearity parameter  $\xi$ . Conventional CKF-based tracking is used as a benchmark to show what can actually be achieved in terms of efficiency and fake rate, and compared to GNN-based tracking and VQE. Eigensolver results are added as a benchmark for VQE approach for a sub-QUBO size of seven.

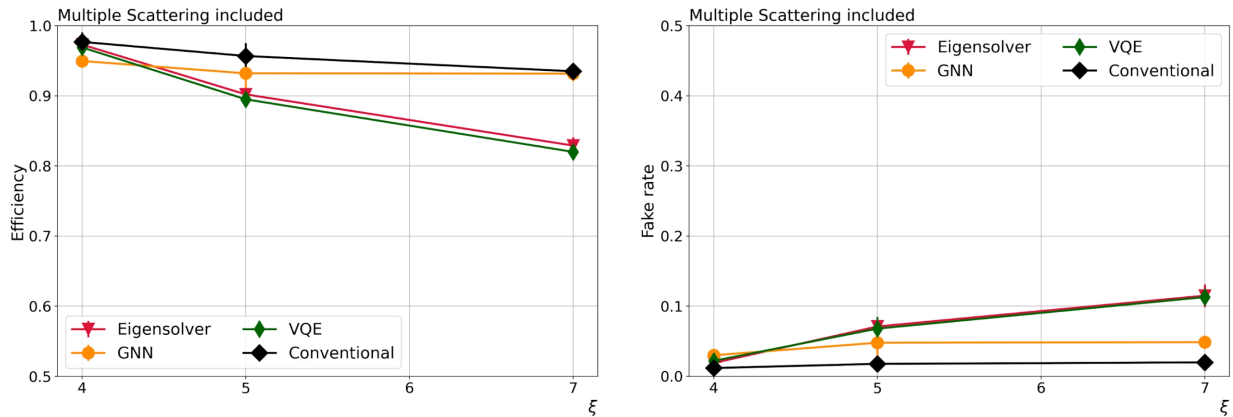


Figure 5: Track reconstruction efficiency and fake rate as a function of  $\xi$ .

CFK-based tracking efficiency decreases with  $\xi$  but is still performant at the highest shown track density at  $\xi = 7$ . GNN-based tracking shows nearly  $\xi$ -independent efficiency. VQE and Eigensolver deteriorate strongly at high  $\xi$  values while being comparable with CKF-based tracking and GNN at  $\xi = 4$ . While GNN is believed to profit from more training examples, hence possibly increasing its performance further, VQE is likely limited by the set of parameters and the size of the sub-QUBOs, therefore both approaches can be further optimized. To investigate the impact of the sub-QUBO size on the performance, only the Eigensolver is used, because simulating VQE for 16 qubits is computationally very costly. In Fig. 6 the impact of the size of the sub-QUBO on the efficiency and fake rate is shown for 1000 tracks, that are closest to the beamline. Increasing the size of the sub-QUBOs from 7 to 16 results in an improvement of the efficiency up to 10% at high  $\xi$ . This indicates, that the available sub-QUBO size is a limiting factor of the optimization algorithm.

Using advanced entanglement structures is a way to improve the results of VQE on the sub-QUBO level. Four different entanglement structures are compared in Fig. 7. Linear entanglement is shown in Fig. 3. Circular entanglement has an additional CNOT entanglement gate from the last to the first qubit. Full entanglement refers to each qubit being entangled with every other qubit. A hamiltonian driven approach is used, if qubits are only entangled if they are representing triplets, which actually have a shared hit, thus an immediate connection. Linear and Hamiltonian driven entanglement show a performance similar to the Eigensolver, which is an upper limit for the performance of the sub-QUBO approach. Full entanglement performs slightly worse, whereas circular entanglement performs very poor. This significant difference in performance is unexpected and will be a subject of further investigations.

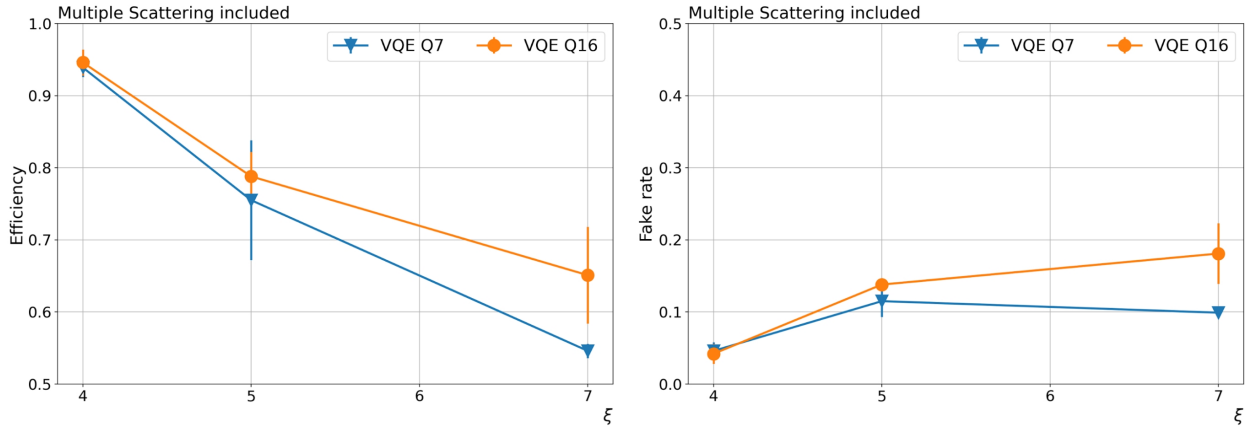


Figure 6: Track reconstruction efficiency and fake rate for 1000 tracks as a function of  $\xi$  for sub-QUBO sizes 7 (Q7) and 16 (Q16).

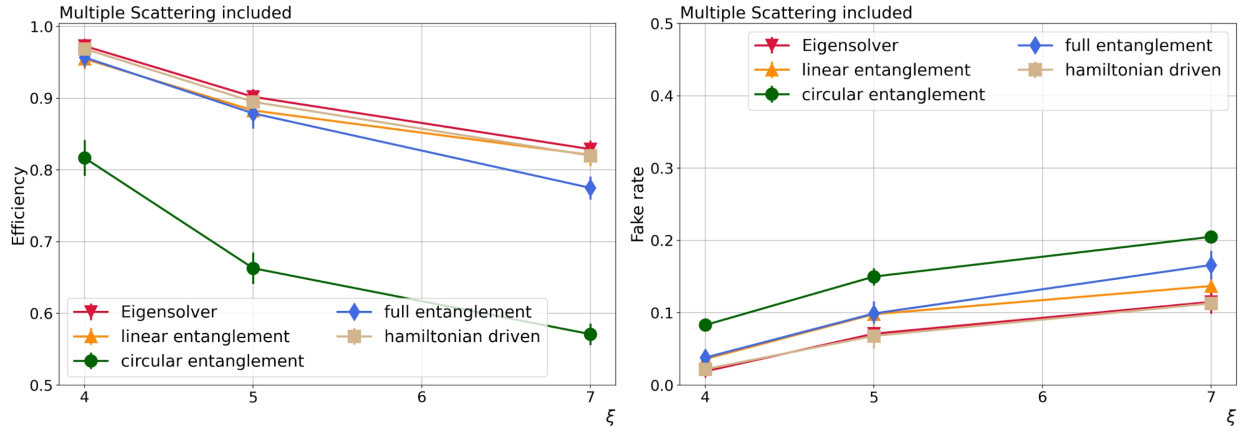


Figure 7: Efficiency and fake rate as a function of  $\xi$ . The Eigensolver result is the upper limit of what can be achieved by employing VQE and using the sub-QUBO subroutine approach.

## 161 6 Conclusions

162 Using a hybrid quantum-classical algorithm for track reconstruction in the LUXE experiment is studied,  
 163 as well as a GNN-based tracking approach. As a benchmark conventional CKF-based tracking is used.  
 164 Currently the performance of the quantum approach is poorer than GNN-based and conventional tracking  
 165 but clues for optimization on the quantum part as well as on the classical part are identified and will be  
 166 investigated in the future. Especially the optimization of the sub-QUBO routine and the possible decoupling  
 167 of its dependency on the sub-QUBO size are strong candidates for major improvements.

## 168 ACKNOWLEDGEMENTS

169 The work by B.H., A.K., F.M., D.S. and Y.Y. was in part funded by the Helmholtz Association - “Innopolis  
 170 Project LUXE-QED”. A.C, K.J. and C.T. are supported in part by the Helmholtz Association - “Innopolis  
 171 Project Variational Quantum Computer Simulations (VQCS)”. L.F. is supported by the U.S. Department  
 172 of Energy, Office of Science, National Quantum Information Science Research Centers, Co-design Center for

173 Quantum Advantage (C<sup>2</sup>QA) under contract number DE-SC0012704, by the DOE QuantiSED Consortium  
 174 under subcontract number 675352, by the National Science Foundation under Cooperative Agreement PHY-  
 175 2019786 (The NSF AI Institute for Artificial Intelligence and Fundamental Interactions, <http://iaifi.org/>),  
 176 and by the U.S. Department of Energy, Office of Science, Office of Nuclear Physics under grant contract  
 177 numbers DE-SC0011090 and DE-SC0021006. S.K. acknowledges financial support from the Cyprus Research  
 178 and Innovation Foundation under project “Future-proofing Scientific Applications for the Supercomputers of  
 179 Tomorrow (FAST)”, contract no. COMPLEMENTARY/0916/0048. This work has benefited from computing  
 180 services provided by the German National Analysis Facility (NAF).

## 181 References

- 182 [1] H. Abramowicz et al., “Conceptual design report for the LUXE experiment,” *Eur. Phys. J.* **230**, 2445-  
 183 2560 (2021) [arXiv:2102.02032].
- 184 [2] L. Funcke, and T. Hartung, B. Heinemann, K. Jansen, A. Kropf, S. Kühn, F. Meloni, D. Spataro, C.  
 185 Tüysüz, Y. Yap, “Studying quantum algorithms for particle track reconstruction in the LUXE experi-  
 186 ment,” (2022) [arXiv:2202.06874].
- 187 [3] H. Gray, “Quantum pattern recognition algorithms for charged particle tracking,” *Phil. Trans. R. Soc*  
 188 **380**, 20210103 (2021) [arXiv:2103.06673].
- 189 [4] T. G. Blackburn, A. J. MacLeod, and B. King, “From local to nonlocal: higher fidelity simulations of  
 190 photon emission in intense laser pulses,” *New J. Phys* **23**, 085008 (2021) [arXiv:2103.06673].
- 191 [5] X. Ai et al., “A Common Tracking Software Project,” [arXiv:2106.13593] (2021).
- 192 [6] S. Farrell et al., “Novel deep learning methods for track reconstruction,” [arXiv:1810.06111] (2018).
- 193 [7] X. Ju et al., “Performance of a geometric deep learning pipeline for HL-LHC particle tracking,” *Eur*  
 194 *Phys. J.* **81**, 876 (2021) [arXiv:2103.06995].
- 195 [8] C. Tüysüz, C. Rieger, K. Novotny, B. Demirköz, D. Dobos, K. Potamianos, S. Vallecorsa, J. Vlimant, and  
 196 R. Forsterter, “Hybrid Quantum Classical Graph Neural Networks for Particle Track Reconstruction,”  
 197 *Quantum Mach. Intell.* **3**, 29 (2020) [arXiv:2103.06995].
- 198 [9] F. Bapst, W. Bhimji, P. Calafiura, H. Gray, W. Lavrijsen, L. Linder, and A. Smith, “A Pattern Recog-  
 199 nition Algorithm for Quantum Annealers,” *Comput. Softw. Big Sci.* **4**, 1 (2020).
- 200 [10] M. Treinish et al., “Qiskit: An Open-source Framework for Quantum Computing,” Zenodo (2022).
- 201 [11] Ken M. Nakanishi and Keisuke Fujii and Syngae Todo, “Sequential minimal optimization for quantum-  
 202 classical hybrid algorithms,” *Phys. Rev. Research* **2**, 043158 (2022) [arXiv:1903.12166].